

# Different Weak C–H···O Contacts in *N*-Methylacetamide–Water System: Molecular Dynamics Simulations and NMR Experimental Study

Rong Zhang, Haoran Li,\* Yi Lei, and Shijun Han

Department of Chemistry, Zhejiang University, Hangzhou 310027, People's Republic of China

Received: January 28, 2004; In Final Form: June 7, 2004

An all-atom *N*-methylacetamide (NMA) model and a refined SPC water model have been adopted for molecular dynamics simulations. <sup>1</sup>H NMR chemical shifts of water, as well as the relative chemical shifts of the NMA methyl group and amide hydrogen atom in the NMA–water system, are measured and calculated over an entire composition range at different temperatures: 308, 323, 338, and 353 K. NMA molecules can act as a hydrogen bonding acceptor or a donor competing with water molecules. Interestingly, the two methyl groups in the NMA molecule are found to have different capabilities in forming weak C–H···O contacts in the mixtures from the radial distribution functions (RDFs). Also, temperature-dependent NMR results of the different methyl groups show excellent agreements with the MD simulations.

## 1. Introduction

The peptide group is an essential repeat unit of protein. Interactions among these peptide groups play an essential role in the structures and properties of proteins and nucleic acids as well as in the behavior of many solvent systems.<sup>1–6</sup> Recently, it has been increasingly recognized that the C–H···O interactions play a significant role in determining the molecular conformation and crystal packing<sup>7–8</sup> in the stabilization of complexes and in the activity of biological macromolecules.<sup>9–11</sup> Weak contacts such as C–H···O exist widely in important biological systems such as nucleic acids, proteins, and carbohydrates, which may be the key to protein folding.<sup>11</sup> A variety of experimental and theoretical methods have been carried out to study the hydrogen bonding of *N*-methylacetamide (NMA) since it is the simplest molecule containing the C=O···H–N characteristic of the peptide bond.<sup>12–35</sup> Spectral measurements such as NMR are highly powerful techniques to investigate structures and interactions in the mixtures.<sup>14–22</sup> Temperature-dependent NMR and quadrupole coupling constants were carried out by Ludwig and co-workers<sup>19,20</sup> to study the structure of liquid NMA by temperature dependence of NMR and IR. Strong cooperative effects were found in the molecular clusters. Molecular dynamics (MD) simulations and other theoretical methods have been widely used in the investigation of the interactions in mixtures.<sup>23–37</sup> More recently, Kwac et al.<sup>23</sup> carried out MD simulations to investigate the amide I mode frequency shift of NMA in both water and deuterated water (D<sub>2</sub>O) solutions. They found that the center frequency and the width of the theoretically calculated absorption spectrum are in excellent agreement with the experimental results. In addition, Buck et al.<sup>26</sup> adopted the MD simulation and energy minimization to study hydrogen bond interactions in the NMA–water mixtures where the potential energy surface is determined by the interactions of entire peptide groups or water molecules rather than by single donor and acceptor groups. Finally, Vargas

et al.<sup>35</sup> found that the C–H···O=C interactions played a crucial role in stabilizing the complexes of several NMA self-association dimers.

To obtain a deeper insight into the NMA–water system, we employed MD simulations and NMR spectra to investigate the intermolecular interactions in the NMA–water mixtures. The radial distribution functions (RDFs), chemical shifts, and the statistics of hydrogen bonding networks were used to reveal the interactions in the NMA aqueous solutions.

## 2. Computational Methods

**2.1. Molecular Models.** Simple rigid potential models were used for both NMA and water. The nonbonded interactions are represented by a sum of the Coulomb and Lennard-Jones terms with eq 1

$$E_{ab} = \sum_i \sum_j^{onb} [q_i q_j e^2 / r_{ij} + 4\epsilon_{ij} (\sigma_{ij}^{12} / r_{ij}^{12} - \sigma_{ij}^6 / r_{ij}^6)] f_{ij} \quad (1)$$

where  $E_{ab}$  is the interaction energy between molecules a and b. Standard combining rules are used via eq 2.

$$\sigma_{ii} = (\sigma_i \sigma_{jj})^{1/2} \quad \epsilon_{ij} = (\epsilon_i \epsilon_{jj})^{1/2} \quad (2)$$

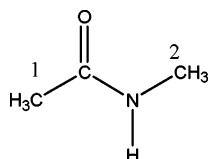
The same expression is used for intramolecular nonbonded interactions between all pairs of atoms ( $i < j$ ) separated by three or more bonds. Furthermore,  $f_{ij} = 1.0$  except for intramolecular 1,4 interactions for which  $f_{ij} = 0.5$ . For water molecule and the NMA molecule, a refined SPC model<sup>38,39</sup> and an OPLS-AA (optimized potentials for liquid simulations—all atom) model<sup>40,41</sup> are performed. Table 1 lists the potential parameters for the pure components. The structure of the NMA molecule is displayed in Scheme 1.

**2.2. Simulation Details.** MD calculations were carried out using a modified TINKER 4.0 molecular modeling package.<sup>42</sup> The simulations were performed in the *NPT* ensemble at  $T = 308$  K and  $P = 1$  atm with a total of 512 molecules. Periodical boundary conditions were used together with a sphere cutoff. The SETTLE algorithm was used to constrain the water

\* Corresponding author: Fax: +86-571-8795-1895 E-mail address: lihr@zju.edu.cn.

**TABLE 1: Potential Parameters for SPC Refined Water and NMA**

atom	$\sigma$ (Å)	$\epsilon$ (kJ/mol)	$q$ (e)
SPC (refined)			
OW	3.1410	0.1554	−0.8068
HW	0.0000	0.0000	0.4034
NMA			
C (C=O)	3.7500	0.1050	0.5000
C <sub>1</sub> (C–CH <sub>3</sub> )	3.5000	0.0660	−0.1800
C <sub>2</sub> (N–CH <sub>3</sub> )	3.5000	0.0660	0.0200
H (N–H)	0.0000	0.0000	0.3000
O	2.9600	0.2100	−0.5000
N	3.2500	0.1700	−0.5000
HC <sub>1</sub> (C–CH <sub>3</sub> )	2.4200	0.0150	0.0600
HC <sub>2</sub> (N–CH <sub>3</sub> )	2.5000	0.0300	0.0600

**SCHEME 1: Structure of NMA Molecule**

geometry, and the SHAKE algorithm was applied to constrain the bond length of NMA. The energies of the initial configurations were minimized using the MINIMIZE program in the TINKER 4.0 package. The time step is 1 fs and configurations were saved every 0.1 ps for analysis. The mixtures were sufficiently equilibrated to ensure that there were no systematic drifts in the potential energies with time. The equilibrations were followed by monitoring the RDFs as well as the fraction of molecules of each species that had a given number of hydrogen bonds. The statistics were collected during the last 100 ps.

**2.3. Definitions.** An analysis of hydrogen bonding networks is adopted to gain deeper insight into the aqueous structures. Here, a geometric criterion used by Luzar and Chandler has been performed,<sup>43</sup> such as a typical criterion of neat water:  $R$  ( $\text{OW}\cdots\text{HW}$ )  $\leq 2.45$  Å,  $R$  ( $\text{OW}\cdots\text{OW}$ )  $\leq 3.60$  Å, and the angle  $\Phi$  ( $\text{HW}-\text{OW}\cdots\text{OW}$ )  $\leq 30^\circ$ . The geometrical criteria of Lei et al.<sup>11</sup> were used for the C–H···O contact:  $R$  ( $\text{O}\cdots\text{H}$ )  $< 2.8$ ,  $3.0 < R$  ( $\text{O}\cdots\text{O}$ )  $< 4.0$  and the angle  $\Phi$  ( $\text{C}-\text{H}\cdots\text{O}$ )  $> 110^\circ$ .

### 3. Experimental Section

NMR spectra were measured using a Bruker DMX 500 spectrometer operating at 500 MHz at different temperatures with an accuracy of  $\pm 0.1$  °C. A 2-mm capillary tube, in which the deuterated dimethyl sulfoxide ( $\text{DMSO}-d_6$ ) was sealed, was placed at the center of a 5-mm sample tube filled with the chemical shift reference of sodium 2,2-dimethyl-2-silapentane-5-sulfonate (DSS) and the sample solution. The  $^1\text{H}$  NMR spectra of the NMA–water mixtures at the different temperatures 308, 323, 338, and 353 K were measured, respectively.

### 4. Results and Discussions

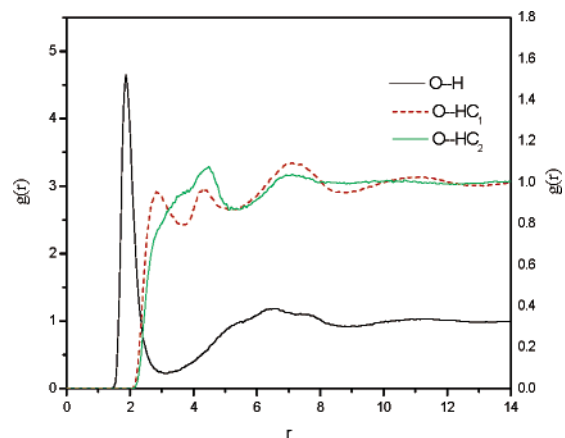
**4.1. Neat NMA and Water.** The density and heat of vaporization of the liquid are important measures of the size of the molecules and the strength of the interaction.<sup>11,44</sup> Calculated properties of neat NMA and water are listed in Table 2, which are compared with experimental values. The calculated densities and heats of vaporization agree well with the experimental values.

The structure of the liquid can be well-characterized by the RDF,  $g(r)[x-y]$ , which gives the probability of finding an atom of type  $y$  at a distance  $r$  from an atom of type  $x$ . The atom types are defined in Table 1. Those  $g(r)$ 's that concern inter-

**TABLE 2: Calculated and Experimental Thermodynamic Properties of Pure Liquids**

liquid	$\Delta H_{\text{vap}}$ (kcal/mol)		$\rho$ (g cm <sup>−3</sup> )	
	cal.	exp.	cal.	exp.
NMA	13.27	13.30 <sup>a</sup>	0.947	0.946 <sup>b</sup>
SPC (refined)	10.33	10.51 <sup>c</sup>	0.983	0.994 <sup>b</sup>

<sup>a</sup> Experimental data are taken from Jorgensen et al.<sup>40</sup> <sup>b</sup> Experimental data are taken from Victor and Harza.<sup>37</sup> <sup>c</sup> Experimental data are taken from Lide.<sup>45</sup>

**Figure 1.**  $g(r)$ 's of neat NMA. Distances are in angstroms. The atom types refer to those in Table 1.

molecular interactions are displayed in Figure 1. The  $g(r)[\text{O}-\text{H}]$  shows two distinct peaks near 1.9 and 6.5 Å, respectively. The first large peak and the short bond distance in the RDF indicate a strong interaction in the carbonyl oxygen atom bonded with the nitrogen hydrogen atom. The  $g(r)[\text{O}-\text{HC}_1]$  presents three distinct peaks near 2.8, 4.3, and 7.1 Å, respectively. Interestingly, the first peak near 2.8 Å of  $g(r)[\text{O}-\text{HC}_2]$  is not obvious. The  $\text{HC}_1$  atom shows better capabilities in forming the weak C–H···O contacts than the  $\text{HC}_2$  atom, which agrees with the geometry in the self-association of a trans-NMA dimer.<sup>35</sup> The first broad peaks of the RDFs also indicate that the intermolecular interactions are likely to include the weak hydrogen bonds as well as other weak interactions such as dipolar interactions and dispersions.

**4.2. NMA–Water Mixtures.** **4.2.1. RDFs. Strong Hydrogen Bonding Interactions.**  $g(r)[\text{OW}-\text{HW}]$  and  $g(r)[\text{O}-\text{HW}]$  show the first distinct peaks near 1.8 Å, which are displayed in Figure 2(a) and (b), respectively. The short distance implies strong interactions of  $\text{OW}\cdots\text{HW}$  and  $\text{O}\cdots\text{HW}$ . The peak locations in RDFs are hardly affected by the concentration of NMA, whereas the peak amplitudes change significantly. The height of the first peak of  $g(r)[\text{OW}-\text{HW}]$  and  $g(r)[\text{O}-\text{HW}]$  increases with  $x_{\text{NMA}}$ , indicating that the NMA and water molecules are apt to be more structured.

**C–H···O Weak Contacts.** It is found that the weak C–H···O contacts cannot be neglected in NMA–water mixtures, as shown in Figure 3. In the water rich region, there is no distinct peak near 2.8 Å of  $g(r)[\text{OW}-\text{HC}_1]$ ,  $g(r)[\text{OW}-\text{HC}_2]$ ,  $g(r)[\text{O}-\text{HC}_1]$ , and  $g(r)[\text{O}-\text{HC}_2]$ , which indicates that both the  $\text{HC}_1$  and  $\text{HC}_2$  atoms are very weak donors in forming the C–H···O contacts. With the increase of  $x_{\text{NMA}}$ , the varieties of RDFs concerning the  $\text{HC}_1$  and the  $\text{HC}_2$  atoms are different. The first distinct peaks near 2.8 Å are observed in  $g(r)[\text{OW}-\text{HC}_1]$  and  $g(r)[\text{O}-\text{HC}_1]$ , and there is still no distinct peak near at the position in  $g(r)[\text{OW}-\text{HC}_2]$  and  $g(r)[\text{O}-\text{HC}_2]$ . This implies that the  $\text{HC}_1$  atom is more favored in forming C–H···O contacts than the  $\text{HC}_2$  atom. The first distinct peaks of  $g(r)[\text{OW}-\text{HC}_1]$

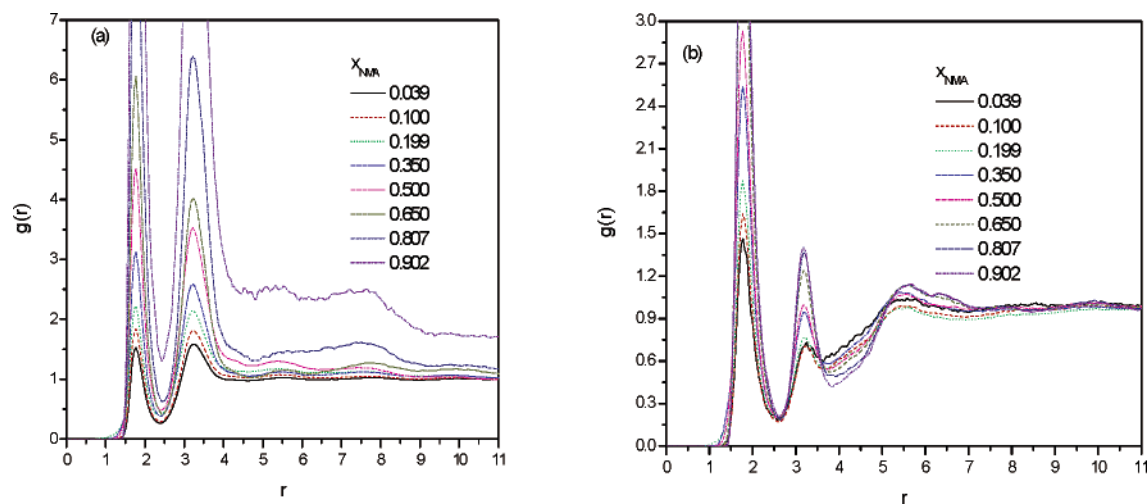


**Figure 2.**  $g(r)$ 's of strong hydrogen bonds in the NMA–water mixtures. (a) OW–HW. (b) O–HW. The atom types refer to those in Table 1.

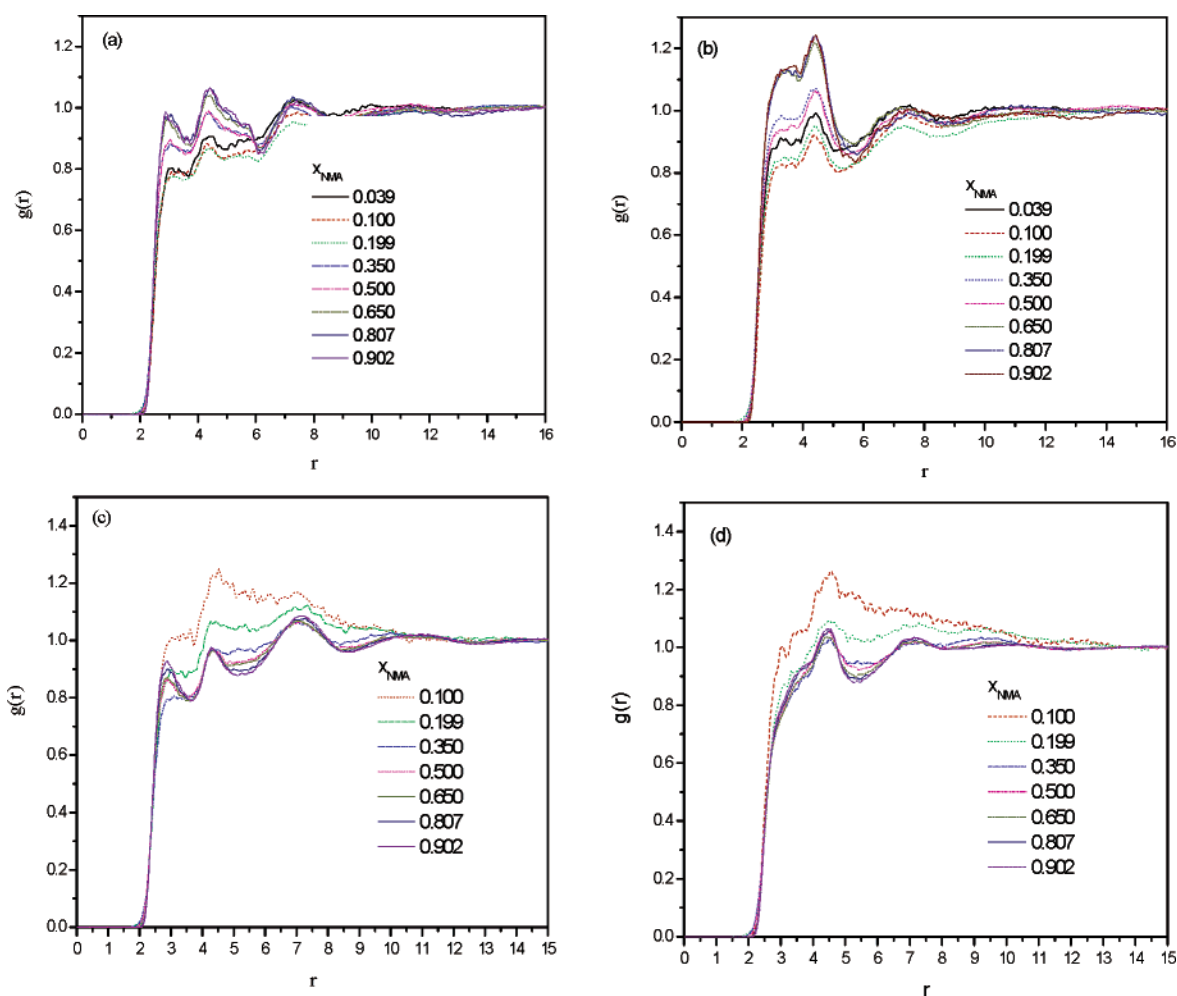


**Figure 3.**  $g(r)$ 's of weak contacts in the NMA–water mixtures. (a) OW–HC<sub>1</sub>. (b) OW–HC<sub>2</sub>. (c) O–HC<sub>1</sub>. (d) O–HC<sub>2</sub>. Distances are in angstroms. The atom types refer to those in Table 1.

and  $g(r)$  [O–HC<sub>1</sub>] indicate that the oxygen atoms of the water or NMA molecule are in close proximity to the HC<sub>1</sub> atom rather than to the HC<sub>2</sub> atom. The carbonyl oxygen atom is a better acceptor than the water oxygen atom, which induces stronger hydrogen bonding interactions.

**4.2.2. Compared with NMR Experiment.** NMR spectroscopy is often used to investigate intermolecular interactions in solution. However, there is still a little spectral data over an entire composition range for aqueous mixtures. It is not easy to

obtain accurate chemical shifts with concentration and temperature dependence. The chemical shifts of some aqueous solutions have been measured by the external reference method.<sup>46–49</sup> Generally, the external reference method, especially the external double reference method, can obtain accurate chemical shifts. However, this method requires a special device and experimental skills. Therefore, the internal reference method has been often adopted to qualitatively measure the chemical shifts of concentration and temperature dependences.<sup>50–52</sup> The internal reference

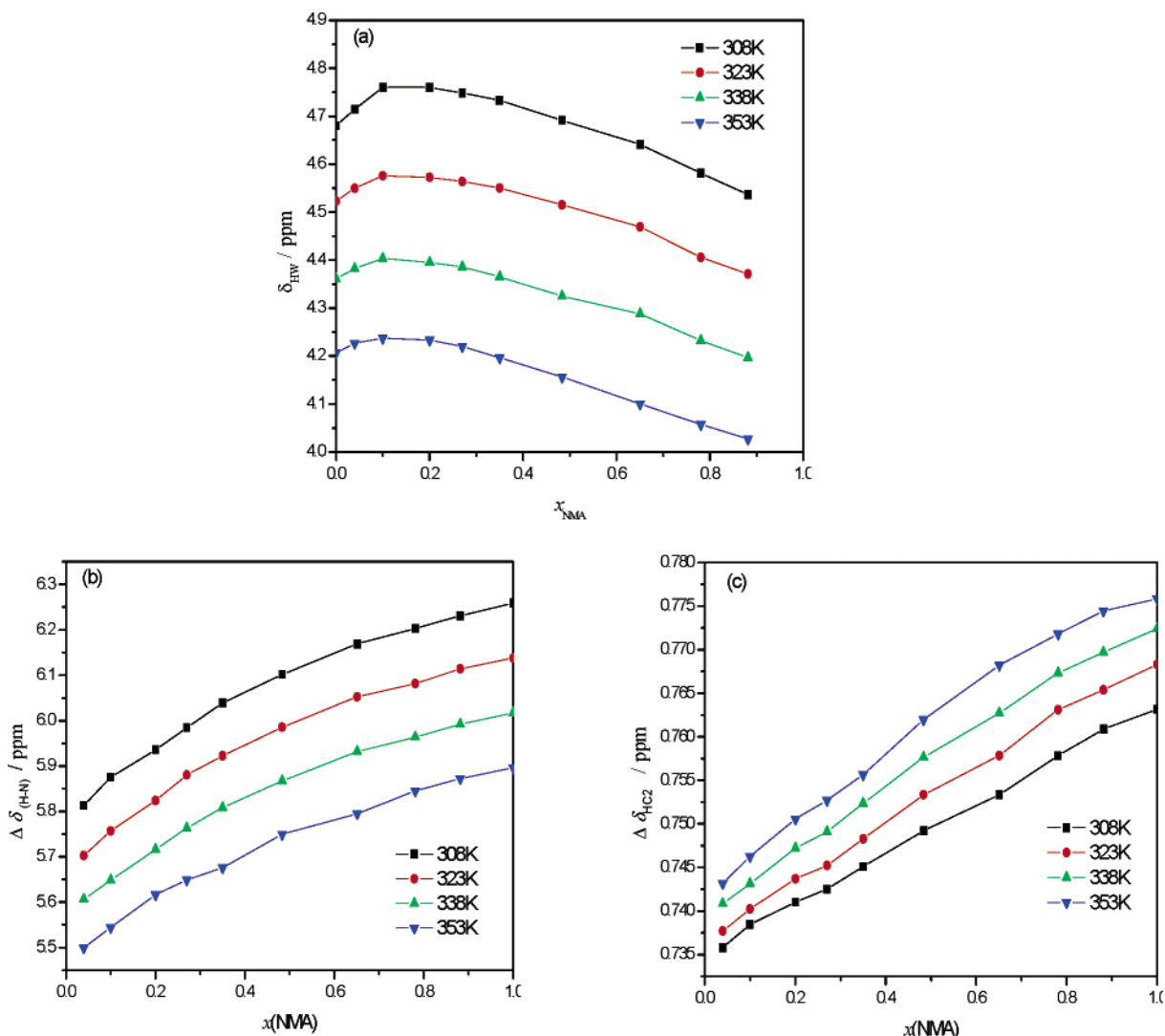


**Figure 4.** (a) Chemical shifts of HW atoms in the NMA–water mixtures against  $x_{\text{NMA}}$  at different temperatures. (b) Relative chemical shifts of amide hydrogen atoms (c) Relative chemical shifts of HC<sub>2</sub> atoms. The atom types refer to those in Table 1.

method was carried out to measure the chemical shifts of the NMA–water mixtures at different temperatures (308, 323, 338, and 353 K).

The chemical shifts of good donors such as water protons greatly change with the concentration, and the effect of the reference can be ignored. However, the chemical shifts of alkyl protons change very little over the whole concentration. The value is about 0.039 ppm of the HC<sub>1</sub> atom, with the internal reference at 308 K. The original chemical data of the two methyl groups with internal reference method are shown in Figure S1 of the Supporting Information. The chemical shifts of alkyl protons can be easily affected by the changes of reference. Due to HC<sub>1</sub>, HC<sub>2</sub>, and the amide hydrogen atom being in the same molecule, the relative chemical shifts compared with the chemical shifts of HC<sub>1</sub> atom ( $\delta_{\text{HC}_1}$ ) are independent of the reference. Thus,  $\delta_{\text{HC}_1}$  is used as the reference standard.

The proton chemical shifts of water ( $\delta_{\text{HW}}$ ) are given in Figure 4a. The  $\delta_{\text{HW}}$  show that the water molecules are apt to be more structured in the water-rich region and the local tetrahedral coordination of water leads to a “breakdown” with  $x_{\text{NMA}}$ . The relative chemical shifts of amide hydrogen atoms ( $\Delta \delta_{\text{H-N}}$ ) and the HC<sub>2</sub> atoms ( $\Delta \delta_{\text{HC}_2}$ ) are shown in Figures 4b and 4c. The varieties of the relative chemical shifts with increasing temperature of the amide hydrogen atoms ( $\Delta \Delta_{\text{H-N}}$ ) and HC<sub>2</sub> atoms ( $\Delta \Delta_{\text{HC}_2}$ ) are also given in Table 3.

**TABLE 3:  $\Delta \Delta \delta_{\text{H-N}}$  (ppm) and  $\Delta \Delta \delta_{\text{HC}_2}$  (ppm) with Temperature Dependence over the Entire Composition Range**

$x_{\text{NMA}}$	$\Delta \Delta \delta_{\text{H-N}}$	$\Delta \Delta \delta_{\text{HC}_2}$
0.040	−0.311	0.008
0.100	−0.330	0.008
0.201	−0.320	0.010
0.270	−0.337	0.010
0.350	−0.361	0.011
0.484	−0.352	0.013
0.651	−0.372	0.015
0.781	−0.357	0.014
0.882	−0.360	0.013
1.000	−0.362	0.013

Hydrogen bonding interactions are sensitive to temperature. Chemical shifts move to high field with increasing temperature. A strong hydrogen bond leads to a greater shift than a weak hydrogen bond. The varieties of the relative chemical shifts with temperature also reflect the relative capabilities of forming hydrogen bonds. Due to the stronger hydrogen bonding capabilities of the amide proton than that of the HC<sub>1</sub> atom, the relative  $\Delta \delta_{\text{H-N}}$  decreases with the increase of temperature. However, the relative  $\Delta \delta_{\text{HC}_2}$  increase with temperature, indicating that the HC<sub>2</sub> atom is a worse donor than the HC<sub>1</sub> atom. The HC<sub>1</sub> atom is more favored in forming C–H···O weak contacts than the HC<sub>2</sub> atom. The variety of  $\Delta \delta_{\text{HC}_2}$  with

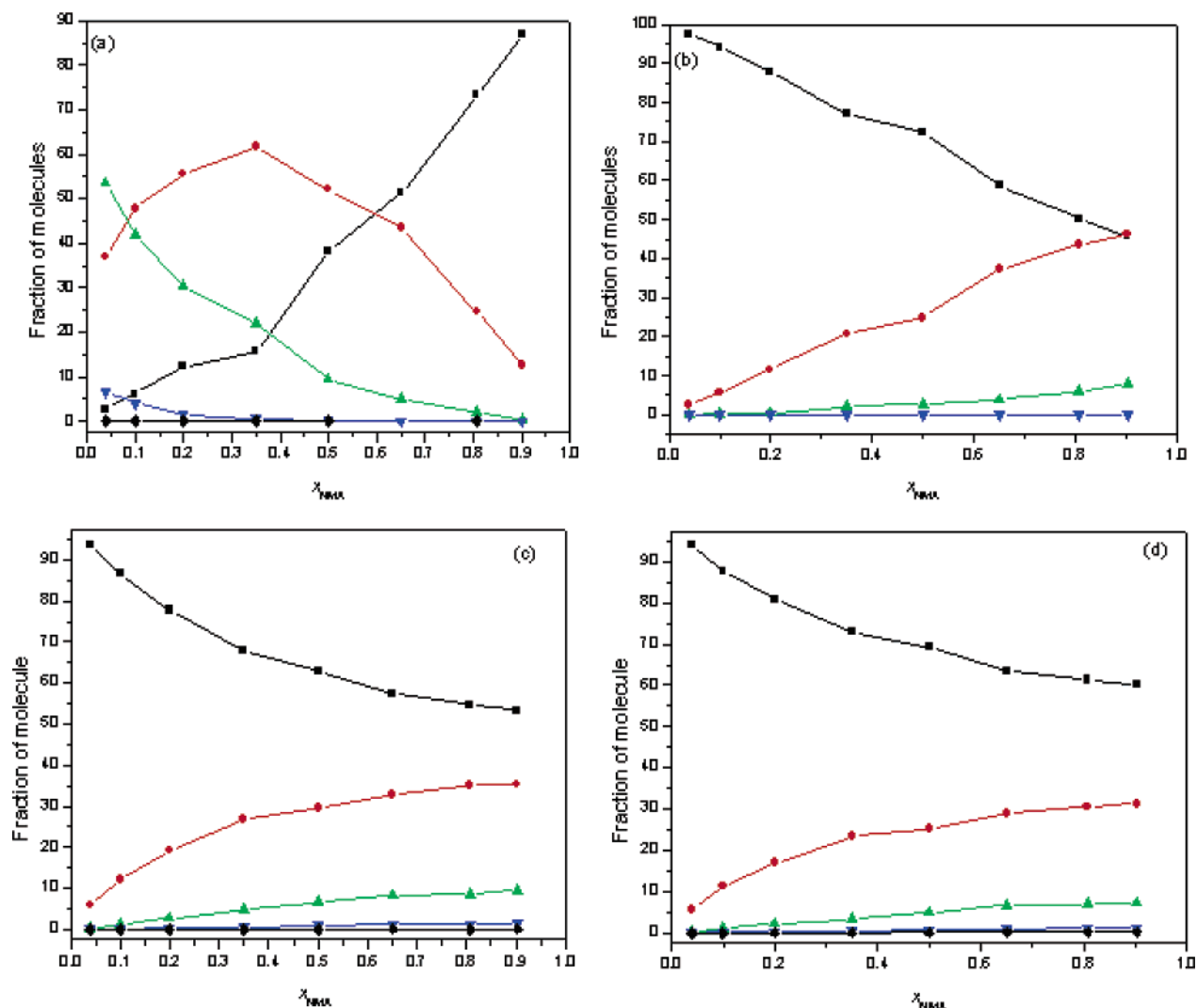


**Figure 5.** (a) Fraction (%) of O atoms accepting zero (■), one (●), two (▲), three (▼), and four (◆) hydrogen bonds to HW atoms. (b) Fraction (%) of OW atoms accepting hydrogen bonds to H atoms. (c) Fraction (%) of OW atoms accepting hydrogen bonds to HC<sub>1</sub> atoms. (d) Fraction (%) of OW atoms accepting hydrogen bonds to HC<sub>2</sub> atoms. The atom types refer to those in Table 1.

temperature is smaller in the water-rich region than that in the NMA rich region, which indicates that the HC<sub>1</sub> atom is more favored in forming C—H···O weak contacts in the NMA-rich region. The NMR experiments and the MD simulations show excellent agreement.

**4.2.3. Hydrogen Bonding Networks.** A detailed analysis of hydrogen bonding networks in the mixtures was carried out to gain deeper information on the aqueous structures. One basic aspect of the hydrogen bonding networks is the probability distribution, describing the number and type of hydrogen bonds that a molecule is engaged with another one. The hydrogen bonds are determined by a geometrical criterion defined in section 2.3. A summary of the statistic of the strong hydrogen bonds of O···HW and OW···H, as well as the weak hydrogen bonds of HC<sub>1</sub>···OW and HC<sub>2</sub>···OW are given in Figure 5.

The carbonyl oxygen atom and the water oxygen atom compete as acceptors of hydrogen bonds. Moreover, the amide hydrogen atom and the water hydrogen atom compete as donors of hydrogen bonds. It is the competition of the four hydrogen-bonding interactions that leads to hydrogen bonding networks in the NMA–water mixtures. For the O···HW hydrogen bonds, the free carbonyl oxygen atoms increase with  $x_{\text{NMA}}$ . However, for the H···OW hydrogen bonds, the free amide hydrogen atoms decrease with  $x_{\text{NMA}}$ . These imply that the water hydrogen atom prefers the carbonyl oxygen atom as acceptors, and the water

oxygen atom prefers its own hydrogen atoms as acceptors. So, the hydrogen-bonded carbonyl oxygen atoms and the free amide hydrogen atoms are predominant in the water rich region. As can be seen in Figure 5(a), the cluster of the carbonyl oxygen atom accepting one proton (O···HW) increases until  $x_{\text{NMA}} \approx 0.35$ , and then decreases with  $x_{\text{NMA}}$ . However, the cluster of the carbonyl oxygen atom accepting two protons decreases with  $x_{\text{NMA}}$ , which indicates that the aggregate of carbonyl oxygen atom accepting two protons of water (NMA·2H<sub>2</sub>O) is more favored in the water-rich region. From Figure 5(c) and 5(d), the aggregates of the OW atom accepting one methyl proton increase rapidly in  $x_{\text{NMA}} < 0.35$ , then increase gently in  $x_{\text{NMA}} > 0.35$ . The number of HC<sub>1</sub>···OW weak hydrogen bonds is larger than that of HC<sub>2</sub>···OW, which also implies the different capabilities in weak C—H···O hydrogen bonds of the two methyl groups. Notice that there is an obvious variety in both the strong hydrogen bonds of O···HW and the weak hydrogen bonds of HC<sub>1</sub>···OW, HC<sub>2</sub>···OW at  $x_{\text{NMA}} \approx 0.35$  of the NMA–water system.

## 5. Conclusions

All-atom MD simulations and NMR spectra have been performed to investigate intermolecular interactions in the NMA–water mixtures. NMA molecules can act as hydrogen



bonding acceptors or competing donors with water molecules, which results in some interesting solvation effects and hydrogen bonding networks. The RDFs from the simulation reveal that the HC<sub>1</sub> atom is more favored in forming C–H···O weak contacts than the HC<sub>2</sub> atom. The internal reference method was performed to measure the chemical shifts over an entire composition range at different temperatures. The varieties of the relative chemical shifts with temperature are used to discuss the effect of temperatures. The temperature-dependent NMR results imply that two methyl groups in NMA molecule have different capabilities in forming the weak C–H···O hydrogen bonds in the mixture, which show excellent agreements with the MD simulations. All-atom MD simulations and NMR spectra are successful in revealing the structures and interactions in the NMA–water mixtures. We expect that these methods are applicable to study a variety of subjects in solution chemistry and biochemistry.

**Acknowledgment.** This work was supported by the National Natural Science Foundation of China (No. 29976035) and Zhejiang Provincial Natural Science of China (No. RC01051).

**Supporting Information Available:** The original chemical shifts data of the two methyl groups of NMA molecule with internal reference method. This material is available free of charge via the Internet at <http://pubs.acs.org>.

## References and Notes

- (1) (a) Manas, E. S.; Getahun, Z.; Wright, W. W.; DeGrado, W. F.; Vanderkooi, J. M. *J. Am. Chem. Soc.* **2000**, *122*, 9883. (b) Langley, C. H.; Allinger, N. L. *J. Phys. Chem. A* **2003**, *107*, 5208.
- (2) Sitkoff, D.; Case, D. A. *J. Am. Chem. Soc.* **1997**, *119*, 12262.
- (3) Kim, K.-Y.; Lee, H.-J.; Karpfen, A.; Park, J.; Yoon, C.-J.; Choi, Y.-S. *Phys. Chem. Chem. Phys.* **2001**, *3*, 1973.
- (4) Akiyama, M. *Spectrochim. Acta, Part A* **2002**, *58*, 1943.
- (5) Kulhánek, P.; Schlag, E. W.; Koča, J. *J. Phys. Chem. A* **2003**, *107*, 5789.
- (6) Ham, S.; Kim, J.; Lee, H.; Cho, M. *J. Chem. Phys.* **2003**, *118*, 3491.
- (7) Green, R. D. *Hydrogen Bonding by C–H Group*; Macmillan: London, 1974.
- (8) Desiraju, G. R.; Steiner, T. *The Weak Hydrogen Bond in Structural Chemistry and Biology*; Oxford University Press: Oxford, 1999.
- (9) Musah, R. A.; Jensen, G. M.; Rosenfeld, R. J.; McRee, D. E.; Goodin, D. B. *J. Am. Chem. Soc.* **1997**, *119*, 9083.
- (10) Gu, Y.; Kar, T.; Scheiner, S. *J. Am. Chem. Soc.* **1999**, *121*, 9411.
- (11) Lei, Y.; Li, H.; Pan, H.; Han, S. *J. Phys. Chem. A* **2003**, *107*, 1574.
- (12) Mabry, S. A.; Lee, B.; Zheng, T.; Jonas, J. *J. Am. Chem. Soc.* **1996**, *118*, 8887.
- (13) Marigliano, A. C. G.; Varetto, E. L. *J. Phys. Chem. A* **2002**, *106*, 1100.
- (14) Herrebout, W. A.; Clou, K.; Desseyn, H. O. *J. Phys. Chem. A* **2001**, *105*, 4865.
- (15) Torii, H.; Tatsumi, T.; Tasumi, M. *J. Raman. Spectrosc.* **1998**, *29*, 537.
- (16) Nandini, G.; Sathyanarayana, D. N. *J. Mol. Struct. (THEOCHEM)* **2002**, *579*, 1.
- (17) Gellman, S. H.; Dado, G. P.; Liang, G.-B.; Adams, B. R. *J. Am. Chem. Soc.* **1991**, *113*, 1164.
- (18) Markham, L. M.; Hudson, B. S. *J. Phys. Chem.* **1996**, *100*, 2731.
- (19) Ludwig, R.; Weinhold, F.; Farrar, T. C. *J. Phys. Chem. A* **1997**, *101*, 8861.
- (20) Ludwig, R.; Reis, O.; Winter, R.; Weinhold, F.; Farrar, T. C. *J. Phys. Chem. B* **1998**, *102*, 9312.
- (21) Torii, H.; Tatsumi, T.; Kanazawa, T.; Tasumi, M. *J. Phys. Chem. B* **1998**, *102*, 309.
- (22) Akiyama, M.; Torii, H. *Spectrochim. Acta, Part A* **1999**, *56*, 137.
- (23) Kwac, K.; Cho, M. *J. Chem. Phys.* **2003**, *119*, 2247.
- (24) Ham, S.; Kim, J.-H.; Lee, H.; Cho, M. *J. Chem. Phys.* **2003**, *118*, 3491.
- (25) Kwac, K.; Cho, M. *J. Chem. Phys.* **2003**, *119*, 2256.
- (26) Buck, M.; Karplus, M. *J. Phys. Chem. B* **2001**, *105*, 11000.
- (27) (a) Zielkiewicz, J.; Mazerski, J. *J. Phys. Chem. B* **2002**, *106*, 861. (b) Zielkiewicz, J. *Phys. Chem. Chem. Phys.* **2000**, *2*, 2925.
- (28) Iuchi, S.; Morita, A.; Kato, S. *J. Phys. Chem. B* **2002**, *106*, 3466.
- (29) Gregurick, S. K.; Chaban, G. M.; Gerber, R. B. *J. Phys. Chem. A* **2002**, *106*, 8696.
- (30) Maple, J. R.; Ewig, C. S. *J. Chem. Phys.* **2001**, *115*, 4981.
- (31) Han, W.-G.; Suhai, S. *J. Phys. Chem.* **1996**, *100*, 3942.
- (32) (a) Cuevas, G.; Renugopalakrishnan, V.; Madrid, G.; Hagler, A. T. *Phys. Chem. Chem. Phys.* **2002**, *4*, 1490. (b) Dixon, D. A.; Dobbs, K. D.; Valentini, J. J. *J. Phys. Chem.* **1994**, *98*, 13435.
- (33) Gao, J.; Freindorf, M. *J. Phys. Chem. A* **1997**, *101*, 3182.
- (34) Vargas, R.; Garza, J.; Dixon, D. A.; Hay, B. P. *J. Am. Chem. Soc.* **2000**, *122*, 4750.
- (35) Vargas, R.; Garza, J.; Friesner, R. A.; Stern, H.; Hay, B. P.; Dixon, D. A. *J. Phys. Chem. A* **2001**, *105*, 4963.
- (36) Chalaris, M.; Samios, J. *J. Mol. Liq.* **2002**, *98–99*, 399.
- (37) Victor, P. J.; Hazra, D. K. *J. Chem. Eng. Data* **2002**, *47*, 79.
- (38) Berweger, C. D.; Gunsteren, W. F.; Müller-Plathe, F. *Chem. Phys. Lett.* **1995**, *232*, 429.
- (39) Mark, P.; Nilsson, L. *J. Phys. Chem. A* **2001**, *105*, 9954.
- (40) Jorgensen, W. L.; Maxwell, D. S.; Tirado-Rives, J. *J. Am. Chem. Soc.* **1996**, *118*, 11225.
- (41) Jorgensen, W. L.; Swenson, C. J. *J. Am. Chem. Soc.* **1985**, *107*, 569.
- (42) Dudek, M. J.; Ramnarayan, K.; Ponder, J. W. *J. Comput. Chem.* **1998**, *19*, 548. Available from <http://dasher.wustl.edu/tinker>.
- (43) Luzar, A.; Chandler, D. *J. Chem. Phys.* **1993**, *98*, 8160.
- (44) Lei, Y.; Li, H.; Han, S. *Chem. Phys. Lett.* **2003**, *380*, 542.
- (45) *CRC Handbook of Chemistry and Physics*, 80th ed.; Lide, D. R., Ed.; CRC Press: Boca Raton, FL, 1999–2000.
- (46) Mizuno, K.; Imafuji, S.; Fujiwara, T.; Ohta, T.; Tamiya, Y. *J. Phys. Chem. B* **2003**, *107*, 3972.
- (47) Mizuno, K.; Kimura, Y.; Morichika, H.; Nishimura, Y.; Shimada, Y.; Maeda, S.; Imafuji, S.; Ochi, T. *J. Mol. Liq.* **2000**, *85*, 139.
- (48) Mizuno, K.; Imafuji, S.; Ochi, T.; Ohta, T.; Maeda, S. *J. Phys. Chem. B* **2000**, *104*, 11001.
- (49) Mizuno, K.; Ochi, T.; Shindo, Y. *J. Chem. Phys.* **1998**, *109*, 9502.
- (50) Dohnal, V.; Tkadlecová, M. *J. Phys. Chem. B* **2002**, *106*, 12307.
- (51) Tkadlecová, M.; Dohnal, V.; Costas, M. *Phys. Chem. Chem. Phys.* **1999**, *1*, 1479.
- (52) Shekaari, H.; Modarress, H.; Hadipour, N. *J. Phys. Chem. A* **2003**, *107*, 1891.